ACS APPLIED MATERIALS & INTERFACES

Letter

www.acsami.org

Use of Magnetic Nanoparticles to Manipulate the Metabolic Environment of Bacteria for Controlled Biopolymer Synthesis

Minsung Park, SuBeom Park, and Jinho Hyun*

Department of Biosystems and Biomaterials Science and Engineering, Seoul National University, Seoul 151-742, Korea

ABSTRACT: Magnetic nanoparticles (MNPs) were covalently immobilized on the surface of *Acetobacter xylinus* and the location of the bacteria was controlled to manipulate bacterial bioactivation. The bacteria were positioned in the middle of an incubation tube by applying an external magnetic field, and the cellulose produced at the different metabolizing locations was characterized by X-ray diffraction, electron microscopy, and differential scanning calorimetry. To the best of our knowledge, this is the first experiment in which MNPs were employed in the control of cell metabolism.

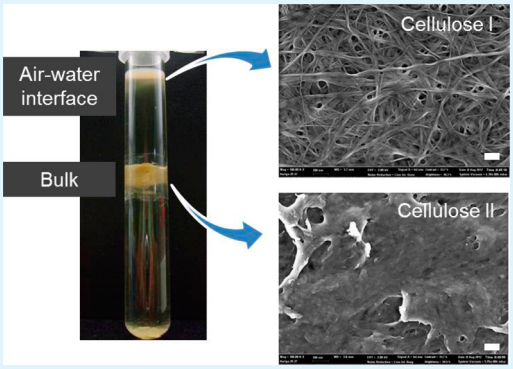

KEYWORDS: *bacterial cellulose, magnetic nanoparticle, position control, biopolymer, cell immobilization, biosynthesis*

Controlling bacterial behavior is very difficult because of their random movements in cell medium. The immobilization of bacterial cells on a surface has been attempted previously.[1,2] However, cell immobilization based on chemical conjugation could be toxic to cells and is restricted to a two-dimensional area.[3,4] Immobilization using a magnetic field has the potential to be more flexible in confining cells as this method is a type of physical control rather than a chemical immobilization of cells onto the surface.[5−11] Using magnetic positioning, cells can retain their three-dimensional motion even while their positions are controlled by applying different magnetic field orientations. This technique is not a method of fixed immobilization but rather a changeable localization. We tested the feasibility of this method by positioning cellulose-producing bacteria in an incubation bath.

Acetobacter xylinus (*A. xylinus*) produces a unique three-dimensional networked structure to protect the bacteria from ultraviolet light on the oxygen-rich air−water interfaces where these bacteria can be found.[12−14] Because most of the bacteria move to the air−water interface and become stuck inside the networked hydrogel, it is difficult to produce cellulose in bulk under static conditions. Production of cellulose in the bulk enables the great diversity in structural and functional properties by incorporating with active or functional materials suspending in solution compared with at the air−water interface. Compared with static culture, agitated culture can produce cellulose throughout the culture media in the form of isolated spheres. It is reported that the cellulose ribbon (cellulose I rich) could be produced at the surface of spheres and continuous shear force during agitation caused the cellulose ribbons to interwine with each other to form the spherical structure. However, bacteria can be separated from the sphere surface for a high shearing force during rotation. In this paper, we used a colloidal suspension of magnetic nanoparticles (MNPs) as an enforcing tool to confine the bacteria to a designated growth region by applying an external magnetic field.

A colloidal suspension of MNPs was prepared in accordance with a previously published coprecipitation method using $FeCl_2{\cdot}4H_2O$ and $FeCl_3{\cdot}6H_2O$.[15] Silica coating of the MNPs was performed with tetraethyl orthosilicate (TEOS) to prevent cytotoxicity. The MNP suspension (1.0g/20 mL) was prepared with a water/ethanol mixture containing ammonia (1.0 mL, 28 wt). One gram of TEOS diluted with 20 mL of ethanol was added dropwise to the dispersion under stirring for 12 h. Silica coated MNPs were collected by magnetic field and washed with ethanol. Transmission electron microscopic (TEM) (JEM 1010, JEOL, Tokyo, Japan) images showed that the MNPs were about 16 nm in diameter. The size of the MNPs coated with silica (silica-MNPs) could be controlled by varying the amount of TEOS. In general, the overall size of the silica-MNPs increased as the amount of TEOS increased. The 50-nm size of silica-MNPs was chosen for the cell positioning in our experiment due to the relatively uniform size and good magnetic response of silica-MNPs.

The surface of the silica-MNPs was further functionalized with aldehyde for conjugation with amine groups on the surface of the bacteria (Scheme 1). First, 1 mL of silica-MNP suspension was added to 20 μL of trimethoxysilane aldehyde in ethanol for 1 h. The aldehyde-functionalized silica-MNPs (CHO-silica-MNPs) were purified by centrifugation at 10 000 rpm for 10 min. To verify successful surface modification and

Received: August 31, 2012
Accepted: October 9, 2012
Published: October 9, 2012

 © 2012 American Chemical Society

Scheme 1. Controlled Positioning of Bacteria Using Magnetic Nanoparticles Modified with Silica[a]

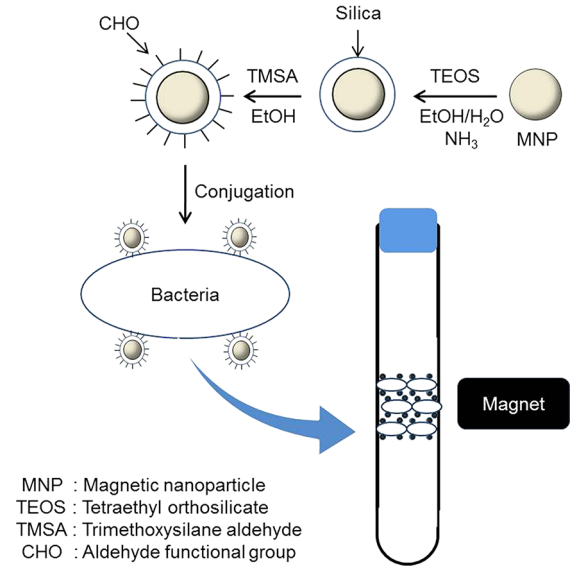

[a]The surface of the silica-coated MNPs was functionalized with aldehyde for conjugation with bacteria. The bacteria conjugated with MNPs were localized by applying an external magnetic field.

functionalization, the infrared spectra of the modified MNP samples were obtained at room temperature (~20 °C) in the wavenumber range of 4000−400 cm^{-1} at a resolution of 2 cm^{-1} using a Fourier transform infrared spectrometer (Thermo Scientific, Nicolet 6700, USA). Si−O−Si fundamental vibration is the source of the strong band at ~1100 cm^{-1}, as shown in Figure 1B. A useful diagnostic band for aldehydes is the C−H stretches at ~2880 cm^{-1} and C═O stretch at ~1750 cm^{-1}, which was observed in the spectrum, thus confirming the successful modification of MNPs into an aldehyde-functionalized surface.[16−18]

To investigate the magnetic behavior of MNPs, magnetization measurements were taken using a superconducting quantum interference device (SQUID)-based magnetometer (MPMS-XL; Quantum Design, USA). Figure 2A shows the hysteresis curves obtained with normal MNPs, silica-MNPs,

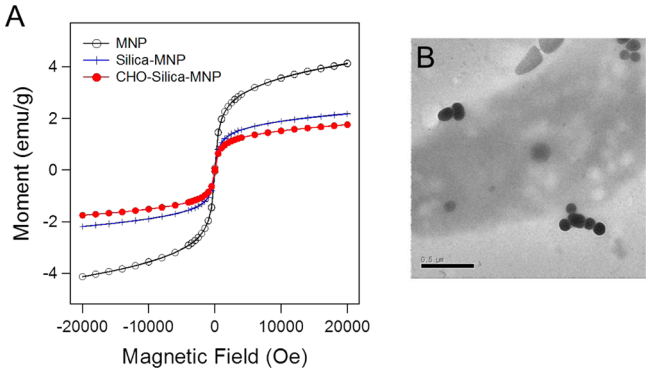

Figure 2. Conjugation of MNPs with bacteria. (A) Magnetization of MNPs after surface modifications and (B) TEM image of bacteria conjugated with MNP. Scale bar = 500 nm.

and CHO-silica-MNPs. The saturation magnetizations of MNPs, silica-MNPs, and CHO-silica-MNPs, as determined by the hysteresis loops, were 4.1, 2.2, and 1.8 emu/g, respectively, which confirmed the characteristic superparamagnetic properties of the nanoparticles (Figure 2A).

The purified CHO-silica-MNPs were resuspended in 1 mL of incubation medium before conjugation with *A. xylinus* (KCCM 40216) obtained from the Korean Culture Center of Microorganisms. One milliliter of CHO-silica-MNPs was added to 1 mL of bacteria-containing medium at room temperature. After 10 min of incubation, the bacteria conjugated with the MNPs (MNP-bacteria) were collected by centrifugation at 2000 rpm for 1 min and then resuspended in 1 mL of incubation medium. The MNP-bacteria were subsequently collected using a magnetic field. It is well-known that the conjugation between aldehyde and amine groups on the cell surfaces occurs rapidly. The presence of MNPs immobilized on the bacterial surface was then confirmed by TEM (Figure 2B). The amount of MNPs conjugated to the bacterial surface was 27 ± 3 particels/cell from TEM images.

The MNP-bacteria were cultured in mannitol medium composed of 2.5% (w/w) mannitol, 0.5% (w/w) yeast extract, and 0.3% (w/w) Bacto Peptone in 50 mL glass tubes. The positions of the MNP-bacteria were easily controlled by using a magnetic field applied to the glass tubes. The magnetic field localized the bacteria in the middle of the medium (5 cm from

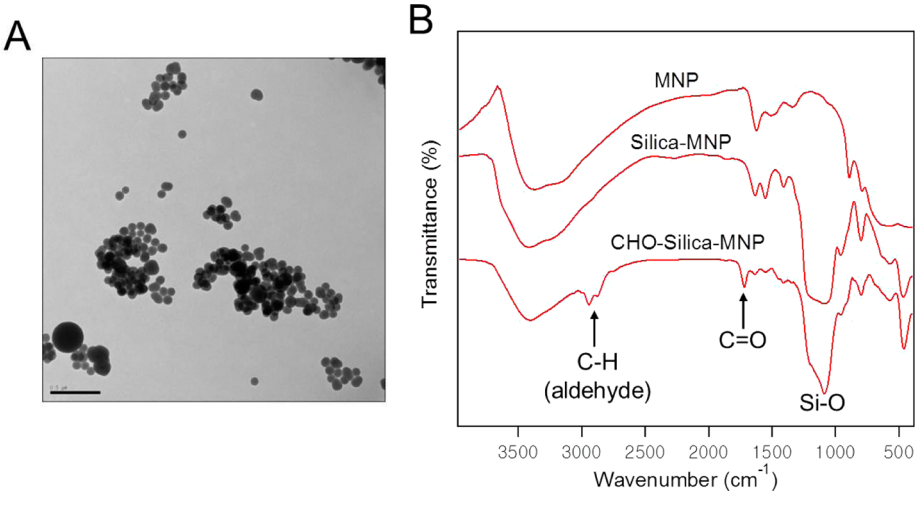

Figure 1. Surface modification of MNPs. (A) TEM image of MNPs coated with silica and (B) FT-IR spectra of MNPs. Scale bar = 500 nm.

dx.doi.org/10.1021/am301839c | *ACS Appl. Mater. Interfaces* 2012, 4, 5114−5117

the air−water interface) without any diffusion of bacteria as long as the magnetic field was applied. The tubes were incubated at 26 °C for 4 days (Scheme 1). Bacterial cellulose (BC) pellicles were formed in the glass tubes at the location at which the magnetic field was applied, as shown in Figure 3A.

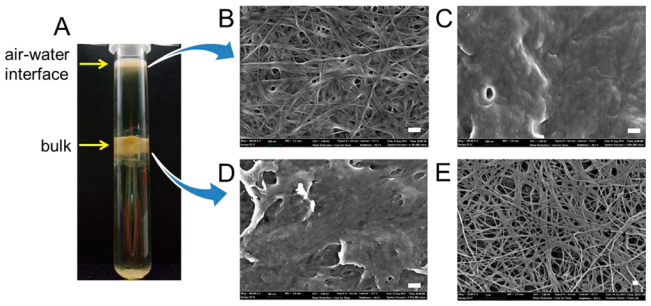

Figure 3. Cellulose production of bacteria. (A) Location of BC produced in the incubation tube. SEM images of cellulose produced by MNP-bacteria at the air−water interface (B) without external magnetic field and (C) with external magnetic field and (D) in the bulk (with external magnetic field). (E) SEM image of cellulose produced by normal bacteria without MNPs at the air−water interface. Scale bar = 200 nm.

Interestingly, when we placed the *A. xylinus* bacteria in a location that they had not previously experienced, they produced cellulose even in the bulk of oxygen deficiency. This indicated that the bacteria were still active and that the protocol presented in this paper can be used to control the position of bacteria or other cells while maintaining their bioactivity and metabolism.

BC biosynthesized in the medium was harvested and purified by boiling the mixture in 1 wt % sodium hydroxide for 2 h at 90 °C, thoroughly washed with distilled water, and then immersed in 1 wt % aqueous sodium hydroxide for 24 h at room temperature in order to eliminate cell debris and remaining culture liquid. The pH was then lowered to 7.0 by repeated washing with distilled water.

A. xylinus normally produces high-crystallinity microfibrils of cellulose I. However, it has been demonstrated that *A. xylinus* can produce cellulose I or cellulose II depending on the culture conditions.[19,20] The two BC pellicle layers formed at the air−water interface (BC-Interface) and the bulk medium (BC-Bulk) were purified and their surface morphologies were compared using field emission scanning electron microscopy (FE-SEM) (S-4300, Zeiss, USA). BC pellicle surfaces coated with platinum are shown in Figures 3B−E. When *A. xylinus* produced cellulose microfibrils in the liquid medium, the cells could move freely, propelling themselves using elongating cellulose microfibrils (cellulose I).[19,21−23] FE-SEM images of BC-Interface showed a ribbon-like uniplanar structure lengthwise with the fiber (Figure 3B, E). In contrast, BC-Bulk showed a nonfibrous structure, as shown in Figure 3D. Comparisons of cellulose produced by bacteria with MNPs and without MNPs at interface demonstrated that the MNPs themself did not influence the morphologies of cellulose (Figure 3B, C). Cell motion was severely restricted by the magnetic field, which affected the type of cellulose produced due to the folding of cellulose chains rather than the typical elongation of cellulose fibrils. As shown in the X-ray diffractogram, it appeared that cellulose I was produced at the air−water interface (Figure 4A) and cellulose II was formed when they were located in the bulk of the medium (Figure 4B). TEM images also confirmed the structural differences between the BCs produced in the different physical environments. BC-Bulk showed a filmlike structure without extension or elongation, whereas BC-Interface showed a ribbon-like planar structure of nanofibers along the fiber axis (Figure 4C, D). The development of cellulose II in BC-Bulk decreased the melting point of BC pellicles because of the reduced availability of hydrogen bonding with cellulose II, which is folded rather than elongated (Figure 4E).

In conclusion, aldehyde-functionalized MNPs were immobilized on the surface of *A. xylinus*, which normally produces cellulose pellicles at the air−water interface of incubation medium. The controlled positioning of MNP-bacteria in the medium was accomplished by applying an external magnetic field. The MNP-bacteria were localized in the middle of the bulk medium, thus physically restricting cell motion. The restriction of bacterial motion in the bulk medium affected the structure of the cellulose and produced a nonfibrous microstructure rich in cellulose II, whereas the bacteria grown without physical restriction produced a ribbon-like microstructure rich in cellulose I. This is a simple method for controlling the position of bacteria by physical enforcement

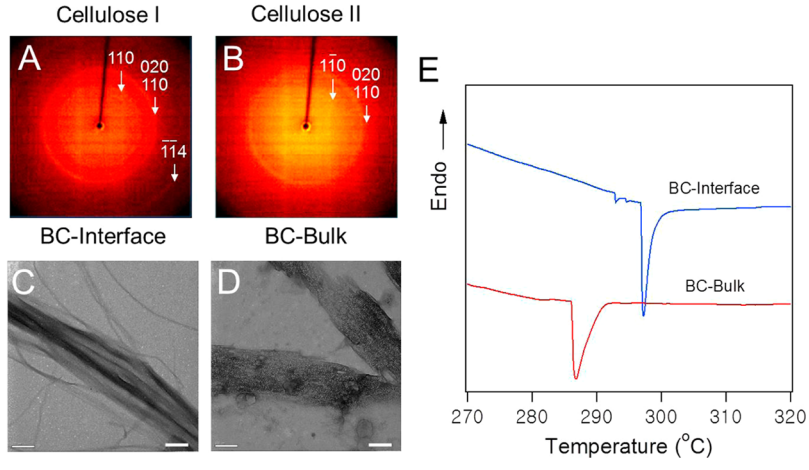

Figure 4. Structural and thermal properties of BCs. X-ray diffractograms of (A) BC-Interface and (B) BC-Bulk. TEM images of (C) BC-Interface and (D) BC-Bulk. (E) Melting point of BCs as characterized by DSC thermograms. Scale bar = 200 nm.

rather than chemical immobilization and without harmful effects on the bioactivity of the cells.

AUTHOR INFORMATION

Corresponding Author
*E-mail: jhyun@snu.ac.kr.

Notes
The authors declare no competing financial interest.

ACKNOWLEDGMENTS

This research was supported by the Basic Science Research Program through the National Research Foundation of Korea funded by the Ministry of Education, Science and Technology (500-20110207). We also acknowledge support from the Research Institute for Agriculture and Life Sciences.

REFERENCES

(1) Johann, R. M. *Anal. Bioanal. Chem.* **2006**, *385*, 408−412.
(2) Nunez, M. J.; Lema, J. M. *Enzyme. Microb. Tech.* **1987**, *9*, 642−651.
(3) Kafi, M. A.; Kim, T. H.; An, J. H.; Choi, J. W. *Biosens. Bioelectron.* **2011**, *26*, 3371−3375.
(4) Marks, K. M.; Nolan, G. P. *Nat. Methods* **2006**, *3*, 591−596.
(5) Bratt-Leal, A. M.; Kepple, K. L.; Carpenedo, R. L.; Cooke, M. T.; McDevitt, T. C. *Integr. Biol.* **2011**, *3*, 1224−1232.
(6) Robatjazi, S. M.; Shojaosadati, S. A.; Khalilzadeh, R.; Farahani, E. V.; Balochi, N. *Bioresour. Technol.* **2012**, *104*, 6−11.
(7) Alhassan, Z.; Ivanova, V.; Dobreva, E.; Penchev, I.; Hristov, J.; Rachev, R.; Petrov, R. *J. Ferment. Bioeng.* **1991**, *71*, 114−117.
(8) Halling, P. J.; Asenjo, J. A.; Dunnill, P. *Biotechnol. Bioeng.* **1979**, *21*, 2359−2363.
(9) Li, Y. G.; Gao, H. S.; Li, W. L.; Xing, J. M.; Liu, H. Z. *Bioresour. Technol.* **2009**, *100*, 5092−5096.
(10) Safarik, I.; Safarikova, M. *J. Chromatogr., B* **1999**, *722*, 33−53.
(11) Shinkai, M. *J. Biosci. Bioeng.* **2002**, *94*, 606−613.
(12) Rani, M. U.; Appaiah, A. *Ann. Microbiol.* **2011**, *61*, 781−787.
(13) Hofinger, M.; Bertholdt, G.; Weuster-Botz, D. *Biotechnol. Bioeng.* **2011**, *108*, 2237−2240.
(14) Ruka, D. R.; Simon, G. P.; Dean, K. M. *Carbohyd. Polym.* **2012**, *89*, 613−622.
(15) Sun, J.; Zhou, S. B.; Hou, P.; Yang, Y.; Weng, J.; Li, X. H.; Li, M. Y. *J. Biomed. Mater. Res., A* **2007**, *80A*, 333−341.
(16) Singh, R. K.; Kim, T. H.; Patel, K. D.; Knowles, J. C.; Kim, H. W. *J. Biomed. Mater. Res., A* **2012**, *100A*, 1734−1742.
(17) Lee, J.; Lee, Y.; Youn, J. K.; Bin Na, H.; Yu, T.; Kim, H.; Lee, S. M.; Koo, Y. M.; Kwak, J. H.; Park, H. G.; Chang, H. N.; Hwang, M.; Park, J. G.; Kim, J.; Hyeon, T. *Small* **2008**, *4*, 143−152.
(18) Setiowaty, G.; Man, Y. B. C. *Food Chem.* **2003**, *81*, 147−154.
(19) Hirai, A.; Tsuji, M.; Horii, F. *Cellulose* **1997**, *4*, 239−245.
(20) Kuga, S.; Takagi, S.; Brown, R. M. *Polymer* **1993**, *34*, 3293−3297.
(21) Shibazaki, H.; Saito, M.; Kuga, S.; Okano, T. *Cellulose* **1998**, *5*, 165−173.
(22) Brown, R. M.; Willison, J. H. M.; Richardson, C. L. *Proc. Natl. Acad. Sci. U.S.A.* **1976**, *73*, 4565−4569.
(23) Yamanaka, S.; Watanabe, K.; Kitamura, N.; Iguchi, M.; Mitsuhashi, S.; Nishi, Y.; Uryu, M. *J. Mater. Sci.* **1989**, *24*, 3141−3145.